

## A DETAILED CFD SIMULATION OF THE 2003 DAEGU METRO STATION FIRE

MYUNGSUNG LEE\* and NAHMKEON HUR<sup>†,‡</sup>

*\*Department of Mechanical Engineering  
Graduate School, Sogang University  
Seoul 121-742, Korea*

*†Department of Mechanical Engineering  
Sogang University, Seoul 121-742, Korea*

*‡nhur@sogang.ac.kr*

Received 22 March 2012

Accepted 13 June 2012

Published 1 November 2012

The Daegu metro station fire on 18 February 2003 was a tragic accident that claimed 192 lives in South Korea. The fire was set by an arsonist in a stopped train at the Daegu metro station, and spread to another train arriving at the station on the opposite track. The present numerical study aims to reproduce the Daegu metro station fire using a transient 3-D CFD simulation with detailed geometry of the station and tunnels in order to understand the behavior of the smoke and heat responsible for human losses in such accidents. The actual motion of the arriving train was also considered by using a moving mesh technique, and the fire development and CO gas generation were modeled with the enthalpy and scalar source terms. The evolutions of the temperature and CO gas distributions in the station were obtained in detail from the present simulation. The heat and CO concentrations at some critical locations (such as staircases) were shown and discussed in detail. The results of the present numerical study could provide useful data for future emergency plans of metro stations in case of fire.

**Keywords:** Daegu metro fire; CFD (computational fluid dynamics); fire safety; train-induced wind.

### 1. Introduction

Though a metro system is considered as a safe means of mass transportation in urban areas, the system has an inherent danger that leads to a disaster in case of fire. The first tragic accident that occurred due to fire in a metro station was Couronnes station of Paris metro in 1903.<sup>1</sup> The fire was caused by a short circuit in a motorcar and consequently the station was filled with heavy smoke. A total of 84 people were killed in the station and tunnel due to the smoke. Another historical metro fire was the King's Cross fire killing 31 people in 1987.<sup>2</sup> This fire

occurred in St. Pancras station of London metro due to a match flame on an escalator. The most tragic metro accident due to fire occurred in Baku metro station of Azerbaijan in 1995.<sup>3</sup> This fire is presumed to have been ignited by electrical malfunction. A flash was seen as the train entered the tunnel, followed by the observation of flames enveloping the train. A total of 289 people were killed and 265 people were injured. Most recently, in 2003, another tragic metro fire accident happened in the Daegu metro station of South Korea.<sup>4</sup> The fire was ignited with four liters of gasoline by an arsonist. As the fire

spread to the flammable interiors of the train such as the seats, flooring, and ceiling, toxic gas and dark smoke rapidly filled the train and station. This accident led to 192 deaths and 148 injuries.

To minimize the loss of life from a metro station fire, optimal emergency plans should be established such as the passenger evacuation and ventilation control among others. Since the emergency plans strongly depend upon the fire behavior, detailed information of the fire-driven flow is very important such as the maximum temperature, toxic gas distributions and smoke movement in the metro station during the fire development. A fire experiment in an actual metro station may be the most accurate method to understand the fire behavior. However, the experiment is not practical due to the limited monitoring locations and huge cost. On the other hand, a computational fluid dynamics (CFD) simulation can provide detailed information of the fire-driven flow in metro stations independent of the huge space and complex geometry of the station.

To provide useful information for fire safety in metro stations, several CFD studies have been performed with numerical simulations on the fire-driven flow in the station. Rie *et al.*<sup>5</sup> simulated the heat and smoke propagation in the case of fire on the platform in a metro station in order to evaluate the effect of a jet fan system on smoke management. Park *et al.*<sup>6</sup> used the FDS program to examine the effect of ventilation capacity on the heat and smoke movements in the case of 12 MW fire at a kiosk in a metro station. Roh *et al.*<sup>7</sup> conducted a simulation to examine the effects of a platform screen door (PSD) and ventilation system on the fire safety in the Daegu metro station. They showed that the PSD and appropriate ventilation system secured a sufficient time for the complete evacuation (about 400 s). These studies, however, have modeled only the station and trains, which are stopped. Since the geometry of the tunnel and actual motion of trains were not included in the previous studies, the piston effect generated in the tunnel due to a moving train on fire development was not investigated.

In the present study, a transient 3-D CFD simulation was performed to reproduce the Daegu metro station fire with detailed geometry of the station and tunnels considering the actual motion of an arriving train. The arriving train was modeled by using a moving mesh technique, and the fire and CO gas were modeled with enthalpy and scalar source terms. The objective of the present study was to

understand what actually happened in the 2003 Daegu metro station fire.

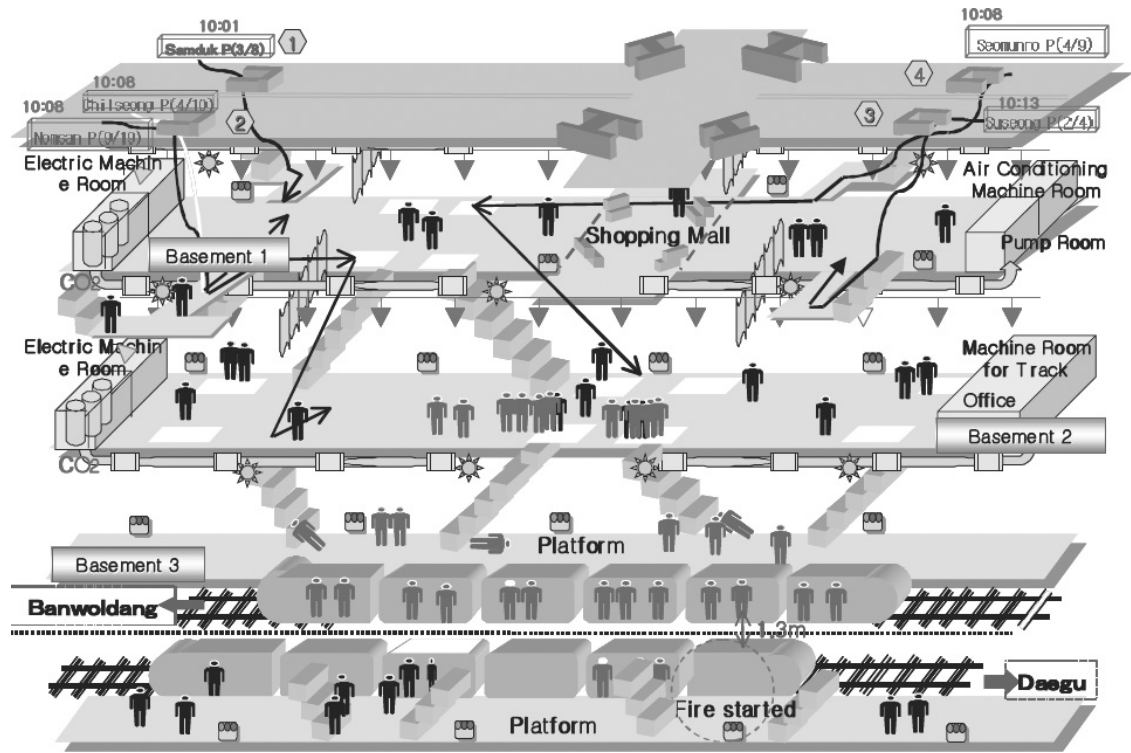
## 2. Summary of the Daegu Metro Station Fire

On 18 February 2003, a train was set on fire by an arsonist at the Daegu metro station in South Korea. Figure 1(a) shows the schematic of the Daegu metro station fire with the location of fire outbreak and casualty distributions. The fire was started inside the 1st carriage of train No. 1079, and then spread quickly throughout the carriage due to highly flammable interior material of the seats, floor, and ceiling. After about 3.5 min, another train had arrived on the opposite track without an appropriate precaution against the fire. This train (No. 1080) cannot escape from the incident station and only a few doors of the train were open due to power failure. Finally, the fire spread from train No. 1079 to the arrived train No. 1080, and killed all passengers trapped inside both trains. Figure 1(b) shows the complete burnt carriages of two trains. As shown in the figure, the distance between two trains is only 1.3 m, showing that the fire can be easily spread between two trains across the track. The burning carriages of trains generated intense heat and poisonous smoke in the station. Since the hot gas and heavy smoke blocked the escape route from the platform to the ground, many passengers were incapacitated from mobility and consequently suffocated on the toxic gas. Details of information on the Daegu metro station fire is outlined in Table 1, including the fire outbreak/extinguished time, fire cause, location of initial fire, and casualty locations. As shown in the table, it is noted that many victims were found not only inside the trains (142 deaths) but also inside the station (50 deaths); a total 50 passengers were dead in basement 2 and 3 of the station. This fact suggests that the understanding of the movement of hot air temperature and the toxic gas in the station is a very important aspect of the metro station fire.

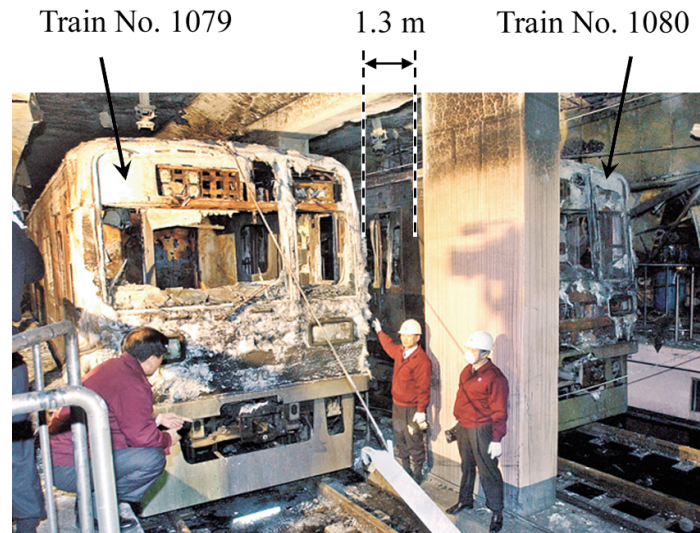
## 3. Numerical Methods

### 3.1. Computational domain and fire modeling

The total computational domain of 3-D CFD simulation for the Daegu metro station fire is shown in



(a)



(b)

Fig. 1. Loss of life and property due to Daegu metro station fire showing casualty distributions (top) and destroyed trains (bottom). Note that the black and grey symbols in the schematic denote injured and dead, respectively. (a) Schematic of Daegu metro station fire showing site of fire outbreak.<sup>8</sup> (b) Burnt carriages of two metro trains.<sup>9</sup>

Fig. 2. The computational domain consists of the Daegu metro station and two tunnels connected to both ends of the station. The tunnels include 700 m of double track ways. The metro station was composed of concrete construction with three basement

levels 200 m in length by 16 m in width. The heights of basement 1, 2 and 3 were 3.15 m, 2.75 m and 5.55 m, respectively. All dimensions of the station were based on the CAD data provided from Daegu Metropolitan Transit Corporation. In the CFD

Table 1. Summary of the Daegu metro station fire.<sup>10</sup>

Date and time of fire outbreak	Date		18 February 2003		
	Fire breaks out		09:53		
	Fire extinguished		13:38		
Fire cause	An arsonist started a fire with gasoline and lighter.				
Site of fire outbreak	The fire was started inside the 1st carriage of train No.1079 and propagated to train No.1080 in the opposite track in basement 3.				
Disaster scale	Death	192	142		Inside trains
			50	11	Basement 2
				39	Basement 3
	Injured	148	Including 10 fire fighters		

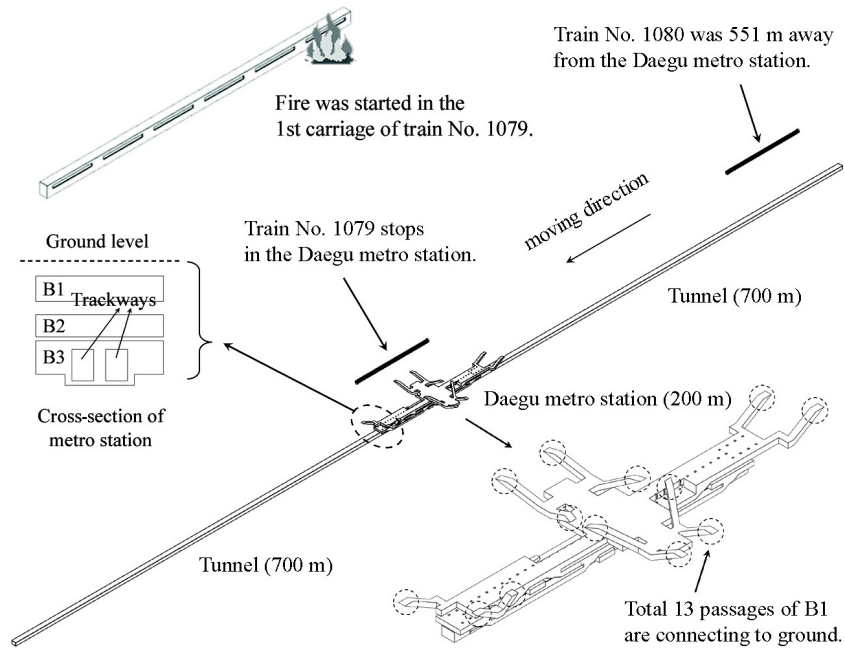


Fig. 2. A computational domain of CFD simulation of Daegu metro station fire. Note that the station consists of three basements, and track ways in the basement 3 are connected to tunnels.

simulation, a total of 13 exits from the station to the ground were set as pressure boundary conditions so that hot air and CO gas could flow out freely. Exits at both ends of the tunnels in basement 3 were also set as the pressure boundary condition. The trains involved in the fire were train Nos. 1079 and 1080 (See Fig. 1(b)). Each train consists of six carriages, which were 2.75 m in width by 3.9 m in height by 18 m in length. As an initial state of the transient CFD simulation, train No. 1079 was stopped at the middle of the station. The fire was started in the 1st carriage of train No. 1079 as shown in Fig. 2. After 2 min 19 s, train No. 1080 departed 551 m away from the station, and arrived at the station 1 min 15 s later. To consider the actual motion of the arriving

train No. 1080, a moving mesh method of STAR-CD V3.26 was used to move grid for the region enveloping the train. Figure 3 shows a detailed floor plan of the three basements (B1, B2, B3) that are connected with staircases denoted by lines in the figure. B1 and B2 are concourses extending north and south. A total of five staircases between B1 and B2 are located on the west side (2a and 2c) and the east side (2b, 2d and 2e). The sizes of staircases are 10 m in length by 2.4 m in width for 2a, 2b, 2c, and 2d (8 m in width for 2e). The metro station has side platforms consisting of west and east platforms in B3. A total of eight staircases between B2 and B3 are located on the west side (3a, 3c, 3e, and 3g) and the east side (3b, 3d, 3f, and 3h). The sizes of



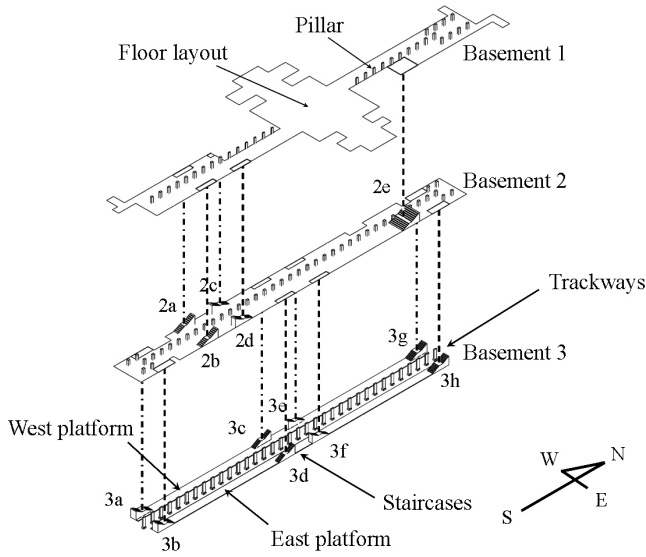


Fig. 3. Details of floor plan of each basement showing the passages between basements denoted by lines. Note that the passages are indexed with basement number.

staircases are 9.5 m in length by 3.2 m in width for 3a, 3b, 3g, and 3h (2.0 m in width for 3c, 3d, 3e, and 3f). The dimensions of cross-section of both tunnels containing the track ways in B3 are 8.22 m in width by 5.55 m in height.

The time history of the Daegu metro station fire is shown in Table 2. The fire broke out at 9:53 a.m. (local time in South Korea), and continued to burn until 13:38 p.m. Considering the time required for passenger evacuation from B3 to ground was predicted at approximately 10 min in a previous study,<sup>11</sup> the present CFD simulation was performed for 20 min after the fire outbreak to obtain sufficient data to predict a safe region against the fire. Figure 4 shows a schematic of fire spread between carriages of trains. The fire spread between carriages was assumed from the previous study<sup>11</sup> that it takes 5 min for a fire burning in one carriage to spread to an adjacent carriage as shown in the figure. The time for the fire to spread across the track from train No. 1079 in the east platform to the 5th carriage of train No. 1080 in the west platform was set at 6 min from the inspection report of the Daegu metro station fire.<sup>11</sup> Figure 5 shows a curve of fire growth and decay adopted at each carriage of the trains. In the present study, a maximum fire size was adopted as 20 MW at 335 s after fire outbreak at each carriage.<sup>12</sup> The CO gas is assumed to have been generated in proportion to the heat release rate (HRR). From the relationship between the HRR and CO gas generations, the maximum concentration of CO gas

Table 2. Time history of the Daegu metro station fire.<sup>10</sup>

Local time	Elapsed time	Event
09:53:11	00:00:00	Fire breaks out in the 1st carriage of train No. 1079
09:55:30	00:02:19	Train No. 1080 departs
09:56:45	00:03:34	Train No. 1080 arrives
09:59:11	00:06:00	Fire spreads from train No. 1079 to train No. 1080
10:27:00	00:33:49	Fire fighters arrive at the platform in basement 3
13:38:00	03:44:49	Fire extinguished

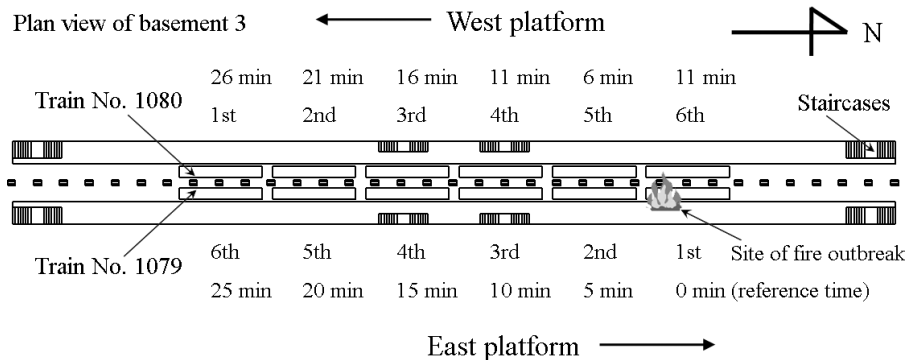


Fig. 4. Schematic of transient fire propagation from 1st carriage of the train No. 1079 in the side of east platform to all carriages of train Nos. 1079 and 1080. Note that the time denotes the beginning of the fire spread at each carriage after fire outbreak.

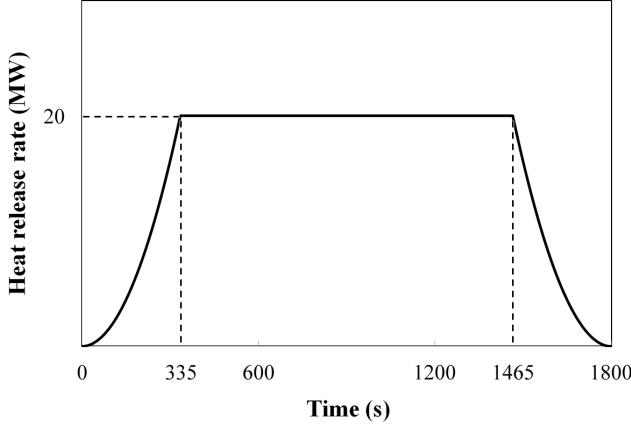


Fig. 5. A curve of fire growth and decay adopted at each carriage of trains. Note that a maximum HRR of 20 MW was imposed at 335 s after the fire outbreak, and the CO gas is assumed to have been generated in proportion to the HRR.

was adopted as 1100 ppm at the maximum HRR of 20 MW.<sup>13</sup>

The computational domain consisting of the station and tunnels was discretized by 11 000 000 cells. A transient 3-D Navier–Stokes solution was obtained with standard  $k - \varepsilon$  model for turbulent flow. A commercial CFD software STAR-CD V3.26 was employed to simulate the flow, temperature, CO concentration fields, and 96 CPUs Linux cluster with Intel Xeon quad-core 2.27 GHz 64 bit processor was used for parallel computation. The computation requires two weeks to simulate 20 min after the fire outbreak.

### 3.2. Governing equations

For the computation of flow, temperature, and CO concentration fields of air in the station and tunnels, four basic balance equations of continuity, momentum, energy and scalar concentration were used. The mass and momentum conservation equations for fluid flow are expressed in Cartesian tensor notation:

$$\frac{\partial \rho}{\partial t} + \frac{\partial}{\partial x_i}(\rho u_i) = 0, \quad (1)$$

$$\begin{aligned} \frac{\partial \rho u_i}{\partial t} + \frac{\partial}{\partial x_j}(\rho u_j u_i - \tau_{ij}) \\ = -\frac{\partial p}{\partial x_i} + g_i(\rho - \rho_0), \end{aligned} \quad (2)$$

where  $\rho$  is the density,  $t$  the time,  $x_i$  the Cartesian coordinates,  $u_i$  the velocity components,  $\tau_{ij}$  the

stress tensor components,  $p$  the pressure. The last term in the momentum equation is for the buoyancy force where  $g_i$  are the gravitational acceleration components,  $\rho_0$  the reference density. The energy conservation is implemented by using the following balance equation:

$$\begin{aligned} \frac{\partial \rho h}{\partial t} + \frac{\partial}{\partial x_j}(\rho h u_j + F_{h,j}) \\ = \frac{\partial p}{\partial t} + u_j \frac{\partial p}{\partial x_j} + \tau_{ij} \frac{\partial u_i}{\partial x_j} + s_h, \end{aligned} \quad (3)$$

where  $h(= \bar{c}_p T - c_p^0 T_0)$  is the static enthalpy,  $F_{h,j}$  the diffusional energy flux,  $s_h$  the enthalpy source,  $\bar{c}_p$  the mean constant-pressure specific heat at temperature  $T$ , and  $c_p^0$  the reference specific heat at temperature  $T_0$ .

The fire was modeled as a volumetric source of enthalpy ( $s_h$ ) without a dedicated combustion model. Many previous studies have shown that this simplified approach is the most practical in terms of low computational cost and its ability to reproduce the overall behavior of fire-induced flow.<sup>14,15</sup> It also has been demonstrated that the same order of accuracy could be achieved in both numerical methods with the fire modeling as the volumetric source and the sophisticated combustion model.<sup>16</sup>

The balance equation of CO concentration (mass fraction of CO gas in the air) is as follows:

$$\begin{aligned} \frac{\partial \rho c}{\partial t} + \frac{\partial}{\partial x_j} \rho c u_j \\ = \frac{\partial p}{\partial t} + u_j \frac{\partial p}{\partial x_j} + \tau_{ij} \frac{\partial u_i}{\partial x_j} + s_c, \end{aligned} \quad (4)$$

where  $c$  is a transported scalar representing the CO gas. The scalar source  $s_c$  was used to model the CO gas generation due to the fire, which was assumed as to be in proportion to the HRR (see Fig. 5).

For the turbulent flow, transport equations for turbulence kinetic energy and dissipation rate were solved by using the standard  $k - \varepsilon$  model considering buoyancy effect as follows:

$$\begin{aligned} \frac{\partial}{\partial t}(\rho k) + \frac{\partial}{\partial x_j} \left[ \rho u_j k - \left( \mu + \frac{\mu_t}{\sigma_k} \right) \frac{\partial k}{\partial x_j} \right] \\ = \mu_t \left( S_{ij} \frac{\partial u_i}{\partial x_j} - \frac{g_i}{\sigma_{h,t}} \frac{1}{\rho} \frac{\partial \rho}{\partial x_i} \right) \\ - \rho \varepsilon - \frac{2}{3} \left( \mu_t \frac{\partial u_i}{\partial x_i} + \rho k \right) \frac{\partial u_i}{\partial x_i}, \end{aligned} \quad (5)$$

$$\begin{aligned}
& \frac{\partial}{\partial t}(\rho\varepsilon) + \frac{\partial}{\partial x_j} \left[ \rho u_j \varepsilon - \left( \mu + \frac{\mu_t}{\sigma_\varepsilon} \right) \frac{\partial \varepsilon}{\partial x_j} \right] \\
&= C_{\varepsilon 1} \frac{\varepsilon}{k} \left[ \mu_t S_{ij} \frac{\partial u_i}{\partial x_j} - \frac{2}{3} \left( \mu_t \frac{\partial u_i}{\partial x_i} + \rho k \right) \frac{\partial u_i}{\partial x_i} \right] \\
&\quad - C_{\varepsilon 3} \frac{\varepsilon}{k} \mu_t \left( \frac{g_i}{\sigma_{h,t}} \frac{1}{\rho} \frac{\partial \rho}{\partial x_i} \right) - C_{\varepsilon 2} \rho \frac{\varepsilon^2}{k} + C_{\varepsilon 4} \rho \varepsilon \frac{\partial u_i}{\partial x_i},
\end{aligned} \tag{6}$$

where  $k$  is the turbulence kinetic energy,  $\mu$  and  $\mu_t$  the molecular and turbulent viscosity,  $\sigma$  the turbulent Prandtl number,  $S_{ij} (= \partial u_i / \partial x_j + \partial u_j / \partial x_i)$  the mean strain tensor, and  $\varepsilon$  the turbulence dissipation rate. The turbulent coefficients  $C_{\varepsilon 1}$  (1.44),  $C_{\varepsilon 2}$  (1.92),  $C_{\varepsilon 3}$  (1.44) and  $C_{\varepsilon 4}$  (−0.33) are used in this model.

#### 4. Results and Discussion

The main causes of death in a metro station fire are severe burns due to fire and high temperature, and suffocation due to toxic gas. As shown in Table 1, the 142 passengers died inside the burning trains because only a few doors were opened due to power failure. Though many passengers escaped the trains caught in the fire, 50 passengers among them were dead on the floor of B2 and B3 due to suffocation by toxic gas (such as CO). It is noted that the temperature and CO gas concentration should be maintained below 60°C and 800 ppm, respectively, for safe passenger evacuation from a fire safety standard.<sup>17</sup> In the present study, the temperature and CO gas concentration in the station were analyzed with this fire safety standard.

The effect of arriving train No. 1080 on the fire development in B3 is shown in Fig. 6. Since the hot temperature is a dominant factor affecting the passenger evacuation in the early stage of a fire, iso-surfaces of 60°C were analyzed as train No. 1080 approached the station. At 100 s after the fire outbreak (see Fig. 6(a)), a fire is developing in the 1st carriage of the stopped train No. 1079 (“A” in Fig. 6). Due to the buoyancy effect, the hot air from the 1st carriage moves toward the ceiling of the B3, as shown in the figure. 150 s after the fire outbreak, it is shown that the iso-surface of 60°C has been formed north and south along with the track ways in B3 as the size of the fire increases. At this point, the burning carriage was only the 1st carriage of train No. 1079 on the east platform, meaning that the region covered with hot air higher than 60°C was

larger on the east platform than on the west platform, as shown in Fig. 6(b). Train No. 1080 departed 139 s after the fire outbreak, and arrived at the station 75 s later; this train was arriving on the west platform, as shown in Fig. 6(c). 200 s after the fire outbreak (see Fig. 6(c)), the flow field in the station seemed to be strongly dependent on the wind induced by the arriving train. As shown in Fig. 6(c), hot air on the ceiling of the west platform flows south toward staircase 3e due to train-induced wind (“B” in Fig. 6). At this time, it is also shown that the temperature field formed on the ceiling of track ways in B3 is becoming perturbed due to the fact that the speed of air becomes higher, which is passing through the narrow passage confined by the upper body of train No. 1080 and the ceiling of track ways in B3. However, this result is not enough to investigate the effect of the arriving train on the overall fire behavior since the event of the arriving train No. 1080 occurred in the early stage of the fire as a low amount of heat was released from the fire source. More examination on the implication of the effect of the moving train will be discussed in this section.

The time history of CO gas distributions after the fire outbreak is shown in Fig. 7 every 5 min in the range of 5 to 20 min. Each iso-surface in the figure denotes 800 ppm of the CO gas concentration, and it shows that the boundary of the iso-surface moves along the wall in the station. At 5 min after the fire outbreak (see Fig. 7(a)), the CO gas vigorously comes from the window of the 1st carriage of train No. 1079. The CO gas moves upward by the buoyancy force due to high temperature near the incident carriage, and then flows along the ceiling above the east platform (“C” in Fig. 7). At 10 min after the fire outbreak (see Fig. 7(b)), the CO gas starts to move from B3 to B2 through the passages of staircases 3e and 3f. Since the CO gas was assumed to have been generated in proportion to the HRR, the CO gas inside the 1st carriage of train No. 1079 was generated with maximum concentration at this time (see Fig. 5). As shown in Fig. 7(b), the height of lower boundary of the iso-surface is decreasing to breathing height, which is 1.5 m above the platform (“D” in Fig. 7), so that passengers may suffer from the toxic CO gas near the incident carriages. After 15 min, more CO gas moves from B3 to B2 through the passages of staircases 3e and 3f, and two CO gas plumes are formed in the passages (“E” in Fig. 7). It is shown that the CO gas has arrived to the ceiling of

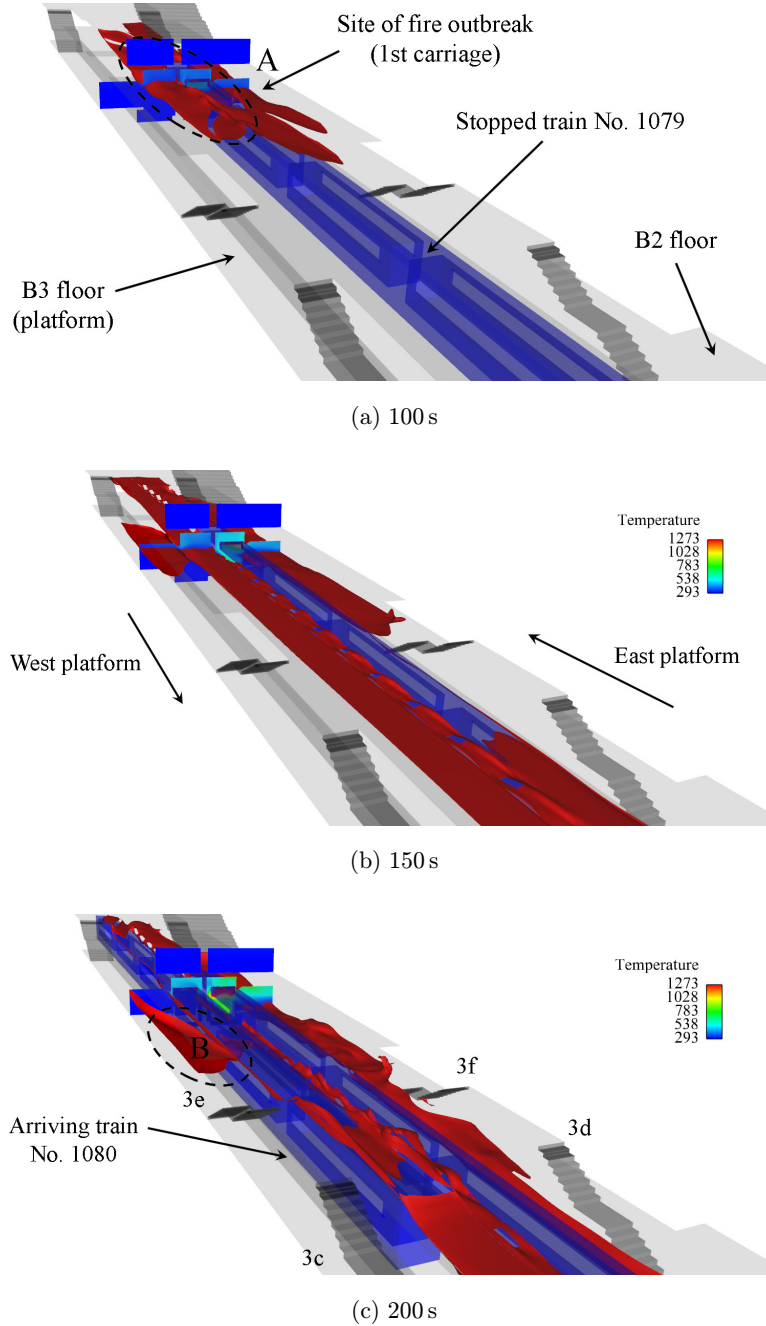


Fig. 6. Effect of an arriving train on the fire development in the station showing iso-surfaces of 60°C temperature at every 50 s after fire outbreak.

B2 through the plumes, and then spreads north on the ceiling of B2. After 20 min, the CO gas moves from B3 to B2 through four passages of staircases 3c, 3d, 3e and 3f. At this time, part of the CO gas starts to flow through the two passages of staircases 3c and 3d (“F” in Fig. 7) while this behavior of CO gas flow was not found at 5, 10, or 15 min after the fire outbreak. The area covered with the CO gas on the

ceiling of B2 is increasing near the passages of staircases 3e and 3f due to the increasing CO gas incoming from B3. It is noted that the height of the lower boundary of 800 ppm CO gas concentration above the platform is decreasing to breathing height throughout B3 after 20 min, which means that passengers could not escape from B3 to B2 at this time due to the suffocating CO gas.



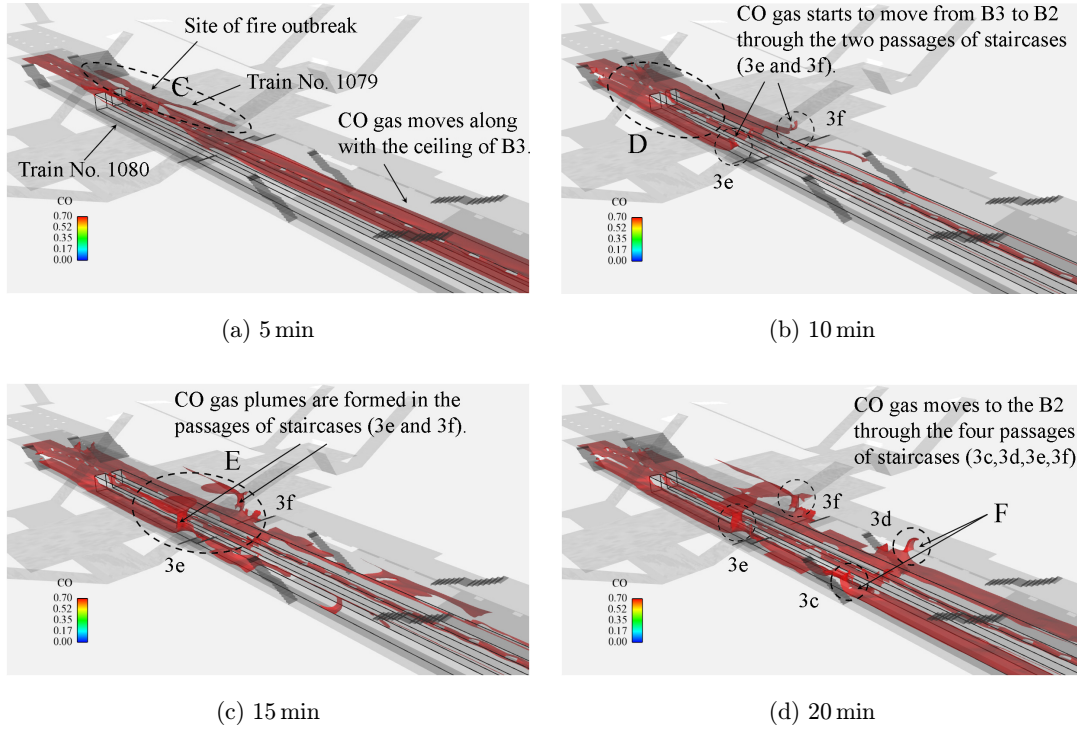


Fig. 7. Transient CO distributions showing the variation of 800 ppm iso-surface of CO gas concentration at every 5 min after the fire outbreak. Note that the edge lines denote the trains.

The maximum temperature predicted in the passages of each staircase in B3 during the fire development is shown in Fig. 8. In the figure, dotted lines and solid lines denote the staircases on the west and east platforms, respectively (see Fig. 3). In the early stage of the fire, the fire size had not reached

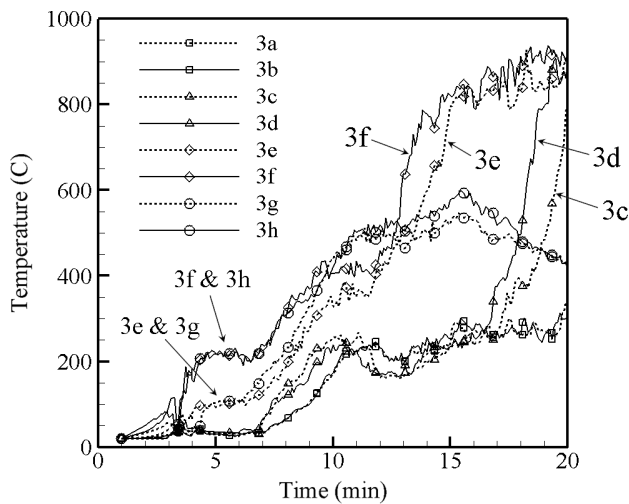


Fig. 8. Time history of maximum temperature predicted in the passages of each staircase in B3 during fire development. Note that hot air flows mainly through staircases 3c, 3d, 3e and 3f, which are located in the middle of the station.

the maximum HRR of 20 MW; the fire started in the 1st carriage of train No. 1079 and reached at the maximum HRR 2 min after the arrival of train No. 1080. As shown in the figure, the temperature is in a relatively low range before train No. 1080 arrived, which suggests that the effect of the train-induced wind is not dominant on the overall fire behavior due to the low HRR from the incident carriage. After train No. 1080 arrived at the station, the fire size increased toward the maximum HRR 20 MW. At this time, the hot air flowed mainly through staircases 3f and 3h on the east platform near the incident 1st carriage of train No. 1079. Portions of hot air also flow through staircases 3e and 3g on the opposite platform. However, the maximum temperature predicted at staircases 3e and 3g were about half of those predicted at 3f and 3h, as shown in the figure. This reveals that the hot air flows mainly through the passages of the staircases on the east platform in the range of 3–7 min after the fire outbreak. It is also noted that the temperature at staircases 3a, 3b, 3c, and 3d is predicted below 50°C until 7 min, which means that a small amount of hot air flowed through these staircases by then. After 7 min, the temperature predicted at all passages in B3 is gradually increasing, since more carriages are

involved in the fire such as the 2nd carriage of train No. 1079 and the 5th carriage of train No. 1080 after 5 and 6 min from the fire outbreak, respectively (see Fig. 4). Though there has been no report of the actual fire behavior in the Daegu metro station fire, the present result seemed reliable since the previous study<sup>4</sup> predicted the maximum temperature at staircase 3f at 10 min after the fire outbreak to be about 400°C by using the FDS, which adopts a complicated combustion model, showing similar order with that of the present study. However, the previous study<sup>4</sup> performed the fire simulation for only 10 min after the fire outbreak, so comparison with results of above 10 min after the fire outbreak could not be conducted. In the present study, it is interesting to find two instant occurrences of rapid increasing temperature in the range of 10 min or more after the fire outbreak; the first rise in temperature occurred at staircases 3e and 3f after 12 min, and the second rise occurred at 3c and 3d after 17 min as shown in the figure. Since staircases 3e and 3f are closer to the location of the fire outbreak, the temperature at these staircases rise ahead of those at 3c and 3d. This temperature jump shown in Fig. 8 agrees well with the predicted transient CO gas distributions shown in Fig. 7. It reveals that the main route of the hot air are staircases 3c, 3d, 3e, and 3f with rapid rise in temperature.

The CO gas concentration at a monitoring point located at the breathing height of each staircase is shown in Fig. 9. Since the CO gas propagation depends on the temperature field, the transient CO gas concentration shows the similar pattern with the predicted transient maximum temperature as shown in Fig. 8. However, the transient CO gas concentration shows slower progress than that of the transient temperature behavior. It is due to the fact that the monitoring location of CO gas concentration is the middle height of each staircase, though the maximum concentration of CO gas was found close to the ceiling height due to the buoyancy effect. In an actual fire, the main cause of the death in the station is not burns due to high temperature but the suffocation due to toxic gas such as CO. Since the passengers must use the staircase for their evacuation, the detailed information of CO gas concentration in the staircase is very important. In Fig. 9, staircases 3d, 3e, and 3f show high concentration of CO gas, which means that many casualties may occur in this region if passengers use these staircases. Since 50 passengers died near the staircases

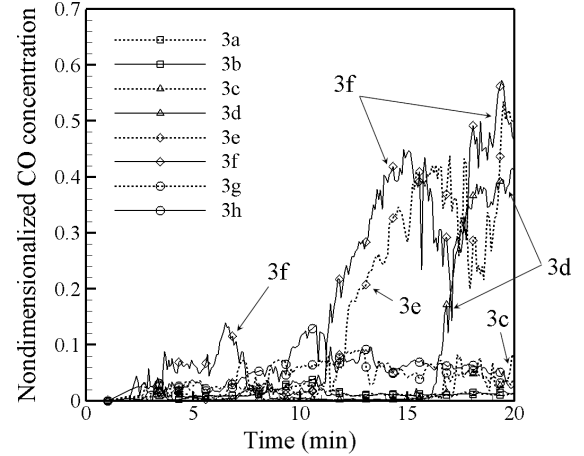


Fig. 9. Time history of CO gas concentration on a monitoring point in the middle of each staircase at 1.5 m above the floor. Note that the CO concentration is nondimensionalized by maximum value of 1100 ppm assumed to have been generated at maximum HRR of 20 MW.

of 3d and 3f on the east platform due to the fire as shown in Fig. 1(a), the numerically predicted hot air and CO gas distributions agree well with the death-occurred region in the actual accident. Few casualties were found on staircases 3c and 3e on the west platform due to the fact that many passengers, who could not escape from train No. 1080 to the west platform, were trapped and killed inside the carriages of train No. 1080, so that staircases 3c and 3e were merely used for passenger evacuation.

## 5. Concluding Remarks

The present study numerically investigated the Daegu metro station fire, which claimed 192 lives in South Korea on 18 February 2003. In order to reproduce the station fire, a transient 3-D CFD simulation was performed with detailed geometry of the station and both tunnels connected to the station. Since the fire was started in one carriage of a stopped train in the station and spread to another train that had arrived 214s after the fire outbreak, a moving mesh method was used to consider the actual motion of the arriving train. The fire growth and CO gas generation were implemented by using the enthalpy and scalar source terms. The maximum heat release rate of 20 MW was adopted at each carriage assuming that it takes 5 min for the fire spread between adjacent carriages. It was found from the results that the effect of the wind induced by arriving train on the fire development was small

since the HRR was low in the early stage of the fire and wind died out rapidly after the arrival of the train. The results also showed that the hot and toxic gas flowed through the passages of staircases between the floors of the station where many casualties were found in actual disaster. The flow route of the CO gas and the height of the fatal level of CO gas concentration above the platform were also shown. The present numerical method could provide useful data for the future emergency evacuation plans of metro stations in case of fire.

## Acknowledgments

This work was financially supported by the National Research Foundation of Korea (NRF) grant No. 20090083510 funded by the Korean government (MEST) through Multi-phenomena CFD Engineering Research Center (ERC) and partially supported by the project from Development of Technology for Fire Safety Evaluation and Prevention Technology for Railway System (T305C1000005-05C010000512).

## References

1. B. Hardy, *Paris Metro Handbook*, 1st edn. (Capital Transport Publishing, 1998).
2. D. Fennell, *Investigation into the King's Cross Underground Fire* (HMSO Publications Centre, 1988), pp. 15–19.
3. J. Hedefalk, B. Wahlstrom and P. Rohlen, Lessons from the Baku subway fire, *Proc. Int. Conf. Safety in Road and Rail Tunnels* (1998), pp. 15–28.
4. M. Tsukahara, Y. Koshiha and H. Ohtani, Effectiveness of downward evacuation in a large-scale subway fire using Fire Dynamics Simulator, *Tunn. Undergr. Space Tech.* **26** (2011) 573–581.
5. D.-H. Rie, M.-W. Hwang, S.-J. Kim, S.-W. Yoon, J.-W. Ko and H.-Y. Kim, A study of optimal vent mode for the smoke control of subway station fire, *Tunn. Undergr. Space Tech.* **21** (2006) 300–301.
6. W. H. Park, D. H. Kim and H. C. Chang, Numerical prediction of smoke movement in a subway station under ventilation, *Tunn. Undergr. Space Tech.* **21** (2006) 304.
7. J. S. Roh, H. S. Ryou, W. H. Park and Y. J. Jang, CFD Simulation and assessment of life safety in a subway train fire, *Tunn. Undergr. Space Tech.* **24** (2009) 447–453.
8. M. Tsujimoto, Issues raised by the recent subway fire in South Korea, *ICUS/INCEDE Newsletter*, Institute of Industrial Science, The University of Tokyo, **3** (2003) 1–3.
9. Maeil Daily Database, Korea (2003).
10. T. H. Kim, Inspection report on the Daegu metro station fire (in Korean), *Proc. Symp. Daegu Metro Station Fire*, The Society of Air-Conditioning and Refrigerating Engineers of Korea (2003), pp. 15–28.
11. Y.-J. Jang, C.-H. Lee, H.-B. Kim and J.-H. Kim, The comparative analysis of fire-driven flow simulation for Dae-gu subway station using FDS and Fluent (in Korean), *Proc. Korean Society for Railway 2008 Autumn Annual Conf.* (2008), pp. 50–55.
12. Transit Development Co. Inc., *Subway Environmental Design Handbook* (US Dept. of Transportation, Urban Mass Transportation Administration, 1976).
13. S.-Y. Kang, K.-H. Kim, Y.-J. Cho, J.-H. Lee and M.-D. Oh, Evacuation environment in a railroad tunnel on fire (in Korean), *Proc. Society of Air-Conditioning and Refrigeration Engineers of Korea 2000 Winter Annual Conf.* (2000), pp. 181–187.
14. K. C. Karki, S. V. Patankar, E. M. Rosenbluth and S. S. Levy, CFD model for jet fan ventilation systems, *Proc. 10th Int. Symp. Aerodynamics and Ventilation of Vehicle Tunnels Principles, Analysis and Design* (2000), pp. 355–380.
15. M. G. Vega, K. M. A. Díaz, J. M. F. Oro, R. B. Tajadura and C. S. Morros, Numerical 3D simulation of a longitudinal ventilation system: Memorial Tunnel case, *Tunn. Undergr. Space Tech.* **23** (2008) 539–551.
16. X. Hue, J. C. Ho and Y. M. Cheng, Comparison of different combustion models in enclosure fire simulation, *Fire Safety J.* **36** (2001) 37–54.
17. Standard for fixed guideway transit and passenger rail systems, NFPA 130, National Fire Protection Association, USA (2000).